Functional Characterization of Monomeric Photosystem II Core Preparations from *Thermosynechococcus elongatus* with or without the Psb27 Protein†

Fikret Mamedov,‡ Marc M. Nowaczyk,§ Anders Thapper,‡ Matthias Rögner,*,§ and Stenbjörn Styring*,‡

Molecular Biomimetics, Department of Photochemistry and Molecular Science, Ångström Laboratory, Uppsala University, SE-751 20 Uppsala, Sweden, and Lehrstuhl für Biochemie der Pflanzen, Ruhr-Universität Bochum, Universitätsstrasse 150, D-44801 Bochum, Germany

Received January 9, 2007; Revised Manuscript Received March 5, 2007

ABSTRACT: Two monomeric fractions of photosystem II (PS II) core pacticles from the thermophilic cyanobacterium *Thermosynechococcus elongatus* have been investigated using flash-induced variable fluorescence kinetics and EPR spectroscopy. One fraction was highly active in oxygen evolution and contained the extrinsic protein subunits PsbO, PsbU, and PsbV. The other monomeric fraction lacked oxygen evolving activity as well as the three extrinsic subunits, but the luminally located, extrinsic Psb27 lipoprotein was present. In the monomeric fraction with bound Psb27, flash-induced variable fluorescence showed an absence of oxidizable Mn on the donor side of PS II and impaired forward electron transfer from the primary quinone acceptor, Q_A. These results were confirmed with EPR spectroscopy by the absence of the "split S_1" interaction signal from $Y_Z^\bullet$ and the $CaMn_4$ cluster and by the absence of the S_2-state multiline signal. A different protein composition on the donor side of PS II monomers with Psb27 was also supported by the lack of an EPR signal from cytochrome c_{550} (in the PsbV subunit). In addition, we did not observe any oxidation of cytochrome b_{559} at low temperature in this fraction. The presence of Psb27 and the absence of the $CaMn_4$ cluster did not affect the protein matrix around Y_D or the acceptor side quinones as can be judged from the appearance of the corresponding EPR signals. The diminished electron transport capabilities on both the donor and the acceptor side of PS II when Psb27 is present give further indications that this PS II complex is involved in the earlier steps of the PS II repair cycle.

Photosystem II (PS II)[1] is a large membrane spanning enzyme in the thylakoid membrane of cyanobacteria, algae, and higher plants that catalyzes the light driven oxidation of water and reduction of plastoquinone. PS II exists both as monomers and dimers and in higher plants, with their highly organized membrane, dimeric complexes dominate in the appressed part of the thylakoid membrane while monomeric forms of PS II dominate in the nonappressed part (*1*, *2*). In cyanobacteria the spatial separation is less pronounced, but both monomer and dimer complexes of PS II can be formed. In general, dimeric PS II is functionally efficient in water oxidation while PS II monomers, at least in higher plants, can be present in both active and nonactive forms. This is thought to reflect events in the photorepair cycle of PS II (*1*, *3*). In cyanobacteria less is known about the functional differences between monomeric and dimeric forms of PS II.

In recent years the three-dimensional structure of PS II has been solved to sequentially higher and higher resolution (up to 3.0 Å) in the thermophilic cyanobacteria *Thermosynechococcus elongatus* (*4*−*6*) and *Thermosynechococcus vulcanus* (*7*) using crystals of PS II core preparations. This has triggered biochemical and spectroscopic studies of PS II in cyanobacterial core preparations to complement the structural knowledge (*8*, *9*). Most of the previously known subunits have been identified in the crystal structure. In addition, the three-dimensional structure has revealed the molecular details of most of the active redox components in PS II including the P680 chlorophylls (Chl), the intermediary acceptor pheophytin, the first quinone acceptor Q_A, and the donor side components Y_D, Y_Z, and the $CaMn_4$ cluster (*4*−*7*). The crystal structure of the PS II complex also contains two cytochromes: the membrane spanning cytochrome (Cyt) b_{559}, which is present in PS II from all organisms (*10*), and Cyt c_{550} (coded by the *psbV* gene) which is only present in thermophilic cyanobacteria (*11*, *12*).

In addition to the protein subunits found in the PS II core, intact PS II is known to contain many more subunits. In PS

† This work was supported from the Swedish Research Council, the EU program SOLAR-H (NEST ADVENTURE 516510), the Knut and Alice Wallenberg Foundation, the Swedish Energy Agency, and the German Research Council (Sonderforschungsbereich 480, project C1).

* To whom correspondence should be addressed. Tel: +46 18 471 65 80. Fax: +46 18 471 68 44. E-mail: stenbjorn.styring@fotomol.uu.se; matthias.roegner@ruhr-uni-bochum.de.

‡ Uppsala University.

§ Ruhr-Universität Bochum.

[1] Abbreviations: *C.*, *Chlamydomonas*; Chl, chlorophyll; Cyt, cytochrome; D1 and D2, core subunits in PS II; DCMU, 3-(3′,4′-dichlorophenyl)-1,1-dimethylurea; β-DM, *n*-dodecyl β-D-maltoside; EPR, electron paramagnetic resonance; HP, high-potential; LED, light-emitting diode; LP, low-potential; OEC, oxygen evolving complex; P680, primary electron donor of PS II; PS II, photosystem II; [PS II monomers/−Psb27], monomeric PS II preparation without the Psb27 subunit but with the PsbO, PsbU, and PsbV subunits; [PS II monomers/+Psb27], monomeric PS II preparation with the Psb27 subunit but without the PsbO, PsbU, and PsbV subunits; Q_A and Q_B, primary and secondary quinone acceptors, respectively, in PS II; *T.*, *Thermosynechococcus*; Tris, tris(hydroxymethyl)aminomethane; Y_D, tyrosine 160 on the D2 subunit; Y_Z, tyrosine 161 on the D1 subunit.

10.1021/bi7000399 CCC: $37.00
Published on Web 04/14/2007

II from cyanobacteria or higher plants there are more than 19 or 25 subunits, respectively, and many of these have been assigned biochemical and biophysical properties (*13*, *14*).

Furthermore, additional factors like PratA (*15*) or the D1 processing peptidase CtpA (*16*) are only transiently bound to the complex during the assembly/repair process and others like IdiA (*17*) only under specific stress conditions. One of these transient subunits is the recently discovered lipid protein Psb27 (*3*, *18*), which is involved in the repair cycle of PS II. It has attracted considerable interest since binding of this subunit seemingly interferes with the water oxidizing complex in cyanobacteria (*3*, *19*) and higher plants (*20*).

Recently, the isolation of monomeric PS II core particles, either containing or lacking the Psb27 subunit, has been achieved (*3*). Careful biochemical characterization of these preparations revealed that a monomeric PS II fraction with high oxygen evolution activity had a normal donor side composition with the PsbO, PsbU, and PsbV subunits while no Psb27 was present; we will refer to this fraction as [PS II monomers/−Psb27]. A clearly distinguishable monomeric PS II fraction that contained bound Psb27 [PS II monomers/+Psb27] was almost devoid of oxygen evolution activity and lacked the PsbO, PsbU, and PsbV subunits. These three extrinsic subunits bind close to the $CaMn_4$ cluster on the lumenal side of PS II and are known to stabilize the structure and function of the OEC. PsbO is the most essential of the three while the presence of PsbU and PsbV is suggested to optimize the rate of O_2 evolution (*21*). EPR spectroscopy also indicated the presence of Mn in the [PS II monomers/−Psb27] fraction, but no Mn was found in the [PS II monomers/+Psb27] (*3*). From ^{15}N pulse label experiments it was possible to show that the [PS II monomers/+Psb27] is an intermediate in the PS II repair cycle. This intermediate was proposed to be formed prior to the incorporation of the $CaMn_4$ cluster in the fully functional oxygen evolving complex (OEC) leading to the formation of the [PS II monomers/−Psb27] (*3*).

It was therefore of interest to characterize this new intermediate, [PS II monomers/+Psb27], with respect to photosynthetic electron transfer and functionality of PS II redox centers and to compare this with the [PS II monomers/−Psb27] fraction where the OEC is fully functional. In this paper we have applied low-temperature EPR spectroscopy and flash-induced variable fluorescence to analyze and compare the function of nearly all redox components in [PS II monomers/−Psb27] and [PS II monomers/+Psb27] from *T. elongatus*.

MATERIALS AND METHODS

Cell Growth. T. elongatus was grown under normal light conditions (∼30 μE) at 55 °C as previously described (*22*).

PS II Core Particle Preparation. His-tagged PS II core particles (10× His fused to the C terminus of the CP43 subunit) from *T. elongatus* were prepared by a treatment with *n*-dodecyl β-D-maltoside (β-DM). The resulting preparation was further divided by column chromatography using a Sepharose fast flow column (Pharmacia) and a UNO Q6 column (Bio-Rad) as in refs *3* and *22*.

This resulted in separation of four fractions of PS II core particles. Fractions 1 and 2 were monomeric, while fractions 3 and 4 were of different dimeric origin. The four core fractions have been described biochemically in ref *3*. The core preparations were suspended in a buffer composed by 20 mM MES, pH 6.5, 20 mM $CaCl_2$, 20 mM $MgCl_2$, 0.5 M mannitol, and 0.03% β-DM, which was used in all further measurements.

Variable Chl a Fluorescence Relaxation Kinetics. Flash-induced increase and subsequent decrease of the variable Chl *a* fluorescence yield were measured using a double modulation fluorometer (PSI Photon Instruments, Brno, Czech Republic). The instrument contained red LEDs for both actinic (30 μs) and measuring (2.0 μs) flashes. Four measuring flashes were applied per decade in the range from 100 μs to 100 s (to 600 s in cases when DCMU was present) after the actinic flash. The sample concentration was 5 μg of Chl/mL in the β-DM buffer. All samples were dark adapted for 5 min at room temperature before the measurement started. When used, the DCMU concentration was 10 μM.

EPR Spectroscopy. Continuous wave EPR spectra were recorded with a Bruker ELEXSYS E500 spectrometer and a standard Bruker ST4102 or a dual mode Bruker DM4116 cavity. Low-temperature measurements were performed using an Oxford-900 cryostat and ITC-4 temperature controller.

In experiments aimed for quantifications of $Y_D^{\bullet}$ the sample was exposed to room light illumination at room temperature for 90 s and thereafter dark adapted for 5 min at room temperature before freezing (*23*−*25*). All spectra measured at this point are considered as dark-adapted EPR spectra. Induction of the split S_1 signal was done as described in Havelius et al. (*26*) by illumination at 6 K directly into the EPR cavity during accumulation of spectra. Induction of the S_2-state multiline signal was done by illumination at 200 K for 6 min as described in Mamedov et al. (*27*) and Miller and Brudvig (*24*). Oxidation of Cyt b_{559} was achieved by illumination at 77 K for 6 min (*24*, *27*). White light from an 800 W projector lamp filtered through a 4 cm $CuSO_4$(aq) filter was used for all illumination protocols. Induction of the Q_A^--Fe^{2+} EPR signal was achieved after incubation in the presence of 50 mM sodium formate for 15 min (at room temperature) and subsequent chemical reduction with 50 mM sodium dithionite (both from 500 mM stock solutions) (*27*−*29*). After 10 min at room temperature the samples were frozen. All additions and incubations were performed in darkness. Analysis of spectra was performed using the Bruker Xepr 2.1 software.

RESULTS AND DISCUSSION

Structural Differences between the Monomeric Fractions. We have earlier presented a thorough biochemical characterization of the two monomeric fractions of PS II core particles (*3*). On a protein level there are clearly distinguishable differences between the two fractions. In the fraction where Psb27 is present [PS II monomers/+Psb27], three subunits on the donor side of PS II are missing (PsbO, PsbU, and PsbV). In contrast, these three subunits are present in the other fraction, [PS II monomers/−Psb27], that does not contain Psb27. Scheme 1 shows these differences in subunit composition. This scheme also summarizes some of the other structural and functional differences between the two fractions, which are described in the following sections.

Scheme 1

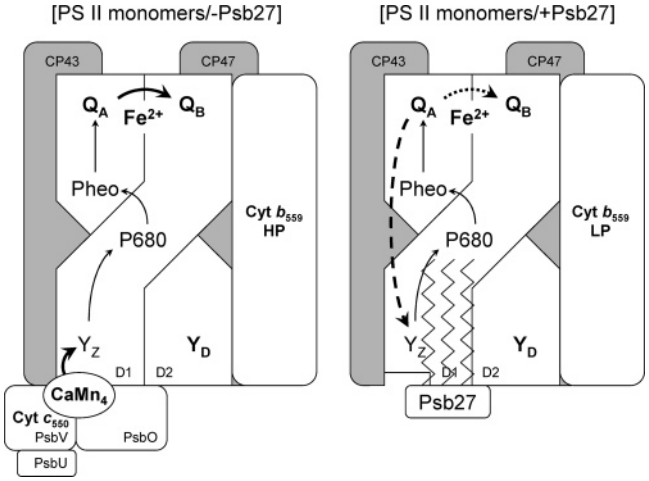

Cytochrome b_{559} has been proposed to mediate cyclic electron transfer in PS II, but it does not take part in linear electron flow. It exists in several redox potential forms, and the status of the PS II complex is influencing the appearance of the different potential forms as well as their redox state (*10*, *30*−*34*). The extrinsic protein PsbV codes for the low-potential (LP) Cyt c_{550} subunit which is present in PS II in *T. elongatus* although it does not participate in the redox events of the water oxidation (*11*, *12*, *35*, *36*). The lack of this protein in [PS II monomers/+Psb27] has been shown by gel electrophoresis (*3*), and our EPR spectra agree well with this. Figure 1A shows EPR spectra recorded in the g_z region of the cytochrome spectrum of 77 K illuminated (full line) and dark-adapted (broken line) samples of the two monomeric fractions. In [PS II monomers/−Psb27] (Figure 1A, top) the EPR spectrum is two times larger than it is in the [PS II monomers/+Psb27] (Figure 1A, bottom). In addition, the illumination at 77 K resulted in further increase of the peak amplitude in the [PS II monomers/−Psb27] while the peak size was unaffected by the illumination in the [PS II monomers/+Psb27]. The larger spectrum in the [PS II monomers/−Psb27] reflects the presence of not only Cyt b_{559} but also Cyt c_{550}, which is known to be oxidized under these conditions (*36*). In this fraction, Cyt b_{559} was not fully oxidized in the dark. Instead, the illumination at 77 K resulted in oxidation of a fraction of Cyt b_{559} (shown as the difference spectrum in Figure 1A, top spectra). In contrast, the smaller spectrum in the [PS II monomers/+Psb27] reflects that this fraction only contains Cyt b_{559}. There was no further oxidation of Cyt b_{559} upon illumination at 77 K, which indicates that the cytochrome was fully oxidized already in the dark.

Figure 1B shows EPR spectra measured at 7 K of the 200 K illuminated (full lines) and dark-adapted (broken lines) samples of the [PS II monomers/−Psb27] (top) and the [PS II monomers/+Psb27] (bottom) fractions. A feature at $g = 6.1$ is visible in both samples but is much more pronounced in the [PS II monomers/+Psb27]. Peaks at this position have been attributed to high-spin Cyt b_{559} (*24*, *37*, *38*). Signals from the oxidized form of the non-heme acceptor side iron could appear in this region (*24*, *39*, *40*) but have been reported to have additional features around $g = 8$ where we do not see any signal in our samples. In the [PS II monomers/−Psb27] the illumination at 200 K resulted in a small increase in the intensity of the $g = 6.1$ feature (top, gray line) whereas no difference could be seen in the [PS II monomers/+Psb27] (bottom, gray line) fraction.

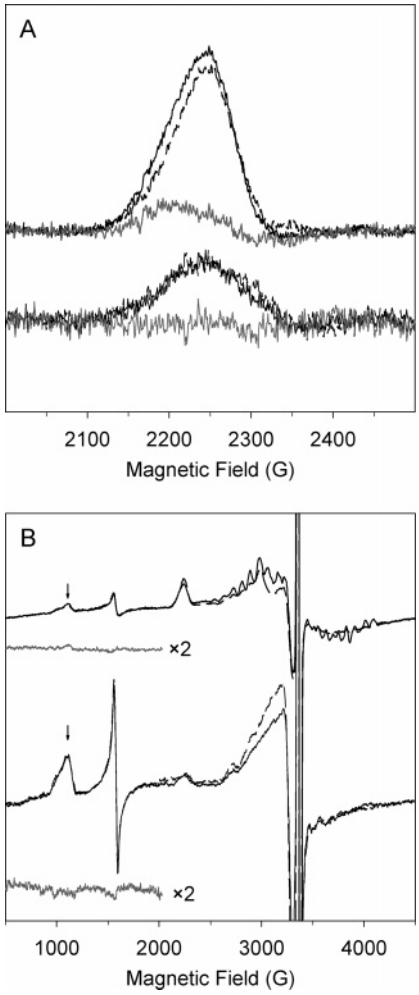

FIGURE 1: (A) EPR spectra of the g_z region of Cyt c_{550} and Cyt b_{559} in the [PS II monomers/−Psb27] (top) and [PS II monomers/+Psb27] (bottom). Dashed spectra were recorded in dark-adapted samples. Full line spectra were recorded after 6 min illumination at 77 K. The spectra are normalized to the $Y_D^{\bullet}$ signal size in the respective sample (from Figure 2). Spectra in gray are the light minus dark difference spectra corresponding to changes in the redox state of Cyt b_{559}. (B) Wide-scan EPR spectra of the [PS II monomers/−Psb27] (top) and [PS II monomers/+Psb27] (bottom). Dashed spectra were recorded in samples exposed to room light illumination at room temperature for 90 s and thereafter dark adapted for 5 min at room temperature. Full line spectra were recorded after 6 min illumination at 200 K. The spectra are normalized to the $Y_D^{\bullet}$ signal size in the respective sample (from Figure 2). Arrows indicate the $g = 6.1$ position. Spectra in gray are the light minus dark difference spectra, magnified two times, corresponding to photoinduced changes in the low-field region of the spectra. EPR conditions: (A) $T = 15$ K, (B) $T = 7$ K; microwave power, (A) 5 mW, (B) 10 mW; modulation amplitude, (A) 15 G, (B) 20 G; microwave frequency, 9.46 GHz.

The g value for the g_z peak of Cyt b_{559} which in the [PS II monomers/+Psb27] is obtained in the absence of Cyt c_{550} is 3.00 (*10*, *24*), which is somewhat higher than the $g = 2.95$ found in tris(hydroxymethyl)aminomethane- (Tris-) washed PS II from *T. elongatus* (*34*). In the presence of the large spectra of oxidized Cyt c_{550} it is more difficult to ascertain the exact g value for the light-induced Cyt b_{559} in the [PS II monomers/−Psb27]. However, it seems clear from the spectrum (Figure 1A, top difference spectrum) that the

Table 1: Comparison of EPR Signals and Number of Chls per Reaction Center for [PS II Monomers/−Psb27] and [PS II Monomers/+Psb27]

PS II monomers	$Y_D^{\bullet}$ [a]	Q_A^--Fe^{2+} [a]	Q_A^--Fe^{2+}-Q_B^- [a]	μmol of O_2 (mg of Chl)$^{-1}$ h^{-1} [b]	Chl/Q_A [b,c]	Q_A/Chl [b−d]
[−Psb27]	100	100	100	∼2900	42	100
[+Psb27]	63	63	63	∼200	64	66

[a] EPR signal sizes normalized to the Chl concentration of the samples; the value for the [PS II monomers/−Psb27] is set to 100 (this work). [b] From ref *3*. [c] Based on absorbance spectra measured at 77 K. [d] Ratio of Q_A centers per Chl (relative value).

g value was higher than for the Cyt b_{559} in the [PS II monomers/+Psb27] (Figure 1A, bottom spectra). A higher *g* value for the high-potential (HP) form than the LP form of Cyt b_{559} has been found in higher plants and algae (*10*, *33*, *41*). Therefore, we assign the photooxidizable fraction of the Cyt b_{559} in the [PS II monomers/−Psb27] to HP Cyt b_{559}. In contrast, both the lower *g* value and the dominance of the oxidized form indicate that Cyt b_{559} was present in the LP form in [PS II monomers/+Psb27].

The dominance of LP Cyt b_{559} in the [PS II monomers/+Psb27] is coherent with the lack of oxygen evolution activity (Table 1) (*3*) and probably reflects the absence of a functional $CaMn_4$ cluster similar to what has been found in PS II from other organisms (*10*, *42*−*44*, and references cited therein). In the [PS II monomers/−Psb27], where HP Cyt b_{559} is present, we observed high oxygen evolution activity (Table 1), indicating a functional $CaMn_4$ cluster (*45*). Consequently, it seems that the Psb27 subunit can only be present when the $CaMn_4$ cluster is absent. In addition, we suggest that the Psb27 subunit is also linked to the redox potential of Cyt b_{559} as indicated in Scheme 1. This agrees well with the proposed role for Psb27 in the repair cycle of PS II and is similar to the situation in higher pants and algae, observed for example during photoactivation of PS II. In the absence of the $CaMn_4$ cluster, Cyt b_{559} is present in the LP form and is converted to the HP form when the oxygen evolving complex (OEC) is activated (*33*, *43*, *44*).

We also recorded the EPR signal from the dark stable $Y_D^{\bullet}$ radical in the [PS II monomers/−Psb27] and [PS II monomers/+Psb27]. Figure 2 shows the EPR spectra of $Y_D^{\bullet}$ induced by an illumination procedure at room temperature which is known to induce the fully oxidized $Y_D^{\bullet}$ (*23*, *25*, *46*). It is clear that the shape of the EPR signal is identical in the two fractions. The shape of the spectral components of an EPR spectrum from a tyrosyl radical reflects the electron spin distribution, the exact molecular orientation of the tyrosine ring plane versus the peptide bond, and the length of the hydrogen bond involving the phenolic proton in Y_D (*47*−*49*). Therefore, the similar spectra show that the binding of Psb27 does not interfere with the molecular environment around Y_D, which is located on the C-helix in the D2 protein close to the lumenal side of the PS II reaction center (*5*, *6*, *50*). Consequently, it is more likely that Psb27 interacts with the D1 side in the PS II reaction center (Scheme 1; note the suggested asymmetric position of Psb27).

Quinone A (Q_A) is a tightly bound plastoquinone that acts as an electron acceptor in PS II. Reduced Q_A^- gives an EPR signal when interacting with the nearby Fe^{2+} ion in PS II (*51*). Formate binds to the acceptor side Fe^{2+}, and this

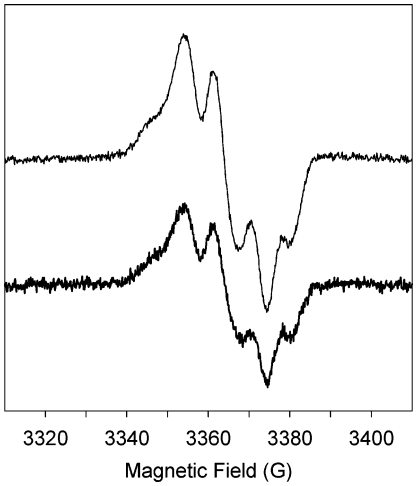

FIGURE 2: EPR spectrum from $Y_D^{\bullet}$ in the [PS II monomers/−Psb27] (top) and [PS II monomers/+Psb27] (bottom). The spectra were recorded in samples exposed to room light illumination at room temperature for 90 s and thereafter dark adapted for 5 min at room temperature before freezing. The spectra are normalized to the Chl concentration of the samples. EPR conditions: $T = 15$ K; microwave power, 1.3 μW; modulation amplitude, 3.5 G; microwave frequency, 9.46 GHz.

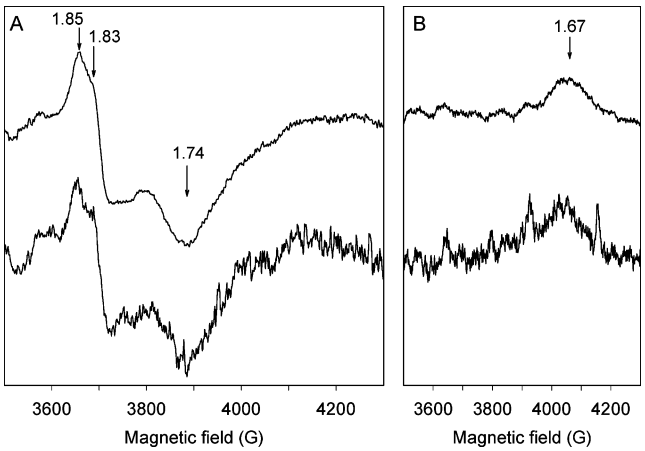

FIGURE 3: (A) The Q_A^--Fe^{2+} EPR signal from [PS II monomers/−Psb27] (top) and [PS II monomers/+Psb27] (bottom). The samples were treated with formate and chemically reduced with dithionite for 10 min (see Materials and Methods). The figure shows difference spectra of reduced minus oxidized samples. (B) Light minus dark difference spectra showing the Q_A^--Fe^{2+}-Q_B^- EPR spectrum from the [PS II monomers/−Psb27] (top) and [PS II monomers/+Psb27] (bottom). The signal was induced by 6 min of illumination at 200 K of a dark-adapted sample. All spectra are normalized to the size of $Y_D^{\bullet}$ in the respective sample. EPR conditions for panels A and B: $T = 4$ K; microwave power, 20 mW; modulation amplitude, 20 G; microwave frequency, 9.46 GHz.

treatment is known to significantly enhance the size of the EPR spectrum (*24*, *28*). Figure 3A shows the Q_A^--Fe^{2+} signal in formate-treated and dithionite-reduced samples of the [PS II monomers/−Psb27] (Figure 3A, top) and the [PS II monomers/+Psb27] (Figure 3A, bottom), normalized to the $Y_D^{\bullet}$ size in the respective sample. An important observation is that the spectra from Q_A^--Fe^{2+} in Figure 3A recorded in the two different fractions have an identical spectral shape. In addition, the relative amplitudes of those spectral features are almost identical in the two fractions. In this respect it is interesting to note that those features have been found to be sensitive to small alterations on the acceptor side of PS II (*39*, *52*, *53*) and in purple bacteria (*54*). Consequently, the

identical spectra in the two preparations clearly show that Psb27 does not alter the structure in the vicinity of the Q_A^- binding site or the acceptor side Fe^{2+}. It is thus unlikely that Psb27 binds anywhere close to these components in PS II, which further substantiates the conclusion that Psb27 is located to the donor side of PS II (*3*) (Scheme 1).

Both the relative size of the $Y_D^\bullet$ signal and the relative amplitude of the formate-treated Q_A^--Fe^{2+} signal can also be used for quantification of PS II in different preparations (*24*, *25*, *28*, *46*). The $Y_D^\bullet$ spectra in Figure 2 are normalized to the Chl concentration in the samples, and double integration of the spectra (Table 1) shows that the $Y_D^\bullet$ signal in the [PS II monomers/−Psb27] is about 50% larger than in the [PS II monomers/+Psb27]. The relative size of the Q_A^--Fe^{2+} signal (peak to trough) normalized to the Chl concentration is also given in Table 1, and it can be observed that Q_A^- is formed in direct proportion to $Y_D^\bullet$ in the two samples. These results should be compared with the PS II reaction center content (on a Chl basis) that was obtained by measuring the $P680^+Q_A^-$-$P680Q_A$ absorbance difference spectra at 77 K in similar preparations (*3*). Table 1 shows that this estimation of Q_A^- in the two fractions is exactly coherent with our measurements of both the $Y_D^\bullet$ and the Q_A^--Fe^{2+} EPR signals. Consequently, we conclude that there is about 50% more chlorophylls per PS II reaction center which are able to reduce Q_A in the [PS II monomers/+Psb27] (ca. 65 Chls per reaction center) than in the [PS II monomers/−Psb27] (ca. 42 Chls per reaction center) (Table 1) (*3*). This could have at least two causes: either there is a larger antenna per PS II center for the [PS II monomers/+Psb27] due to a different stoichiometry in the assembly of the PS II subunits in vivo or there is a loss or incomplete incorporation of Q_A into the D2 subunit in the [PS II monomers/+Psb27] leading also to an incomplete oxidation of Y_D in this fraction.

It can be concluded from these investigations that the Psb27 subunit does not interfere with the D2 protein either in the donor side close to Y_D or on the acceptor side close to Q_A. Furthermore, there seems to be ca. 50% more Chl per Q_A^- or $Y_D^\bullet$ in the [PS II monomers/+Psb27] compared to the [PS II monomers/−Psb27].

Function of the Acceptor Side in PS II. The Q_A^--Fe^{2+} EPR signal in PS II preparations from *T. elongatus* obtained after reduction by dithionite in the presence of formate has not been reported earlier. The spectra in Figure 3A are dominated by a peak with $g = 1.85$, a shoulder with $g = 1.83$, and trough at $g = 1.74$. In nontreated PS II from *T. elongatus* the Q_A^--Fe^{2+} EPR signal has a peak at $g = 1.95$ (*9*). The observation of two forms of the Q_A^--Fe^{2+} EPR signal is thus similar to the situation in PS II preparations from spinach where a $g = 1.90$ signal is observed in nontreated samples and a $g = 1.82$ form in formate/dithionite-treated samples (*29*, *51*). The *g* values for the formate-treated Q_A^--Fe^{2+} signal are slightly higher than reported from spinach (1.82 and 1.69 for the peak and trough, respectively). The shoulder on the low-field peak is not observed in spinach, which could indicate different binding of formate to the acceptor side Fe^{2+} in PS II from *T. elongatus*.

The effect of the Psb27 protein on the electron transfer between Q_A and Q_B has been studied by two methods, EPR spectroscopy and flash-induced variable fluorescence.

Figure 3B shows the light minus dark difference EPR spectra from the two fractions recorded after 6 min illumination at 200 K and normalized to the size of $Y_D^\bullet$ in the respective sample. Both in the [PS II monomers/−Psb27] and the [PS II monomers/+Psb27] the illumination at 200 K resulted in formation of a species with a positive EPR signal at $g = 1.67$. This signal has been assigned to a magnetic interaction signal involving the redox state Q_A^--Fe^{2+}-Q_B^- (*9*, *55*−*58*) and has been observed earlier, using a different illumination protocol, in oxygen evolving preparations from *T. elongatus*. The observation of this signal indicates either that the [PS II monomers/−Psb27] fraction contains a substantial part of PS II with reduced Q_B in the dark-adapted sample or that electron transfer to the second electron acceptor Q_B is possible by photoaccumulation also at temperatures as low as 200 K. Our results here indicate that the same situation applies also in the presence of Psb27 (Figure 3B, lower). In addition, the relative amplitude of the Q_A^--Fe^{2+}-Q_B^- signal is similar between the two fractions to the EPR signals of $Y_D^\bullet$ and Q_A^--Fe^{2+}.

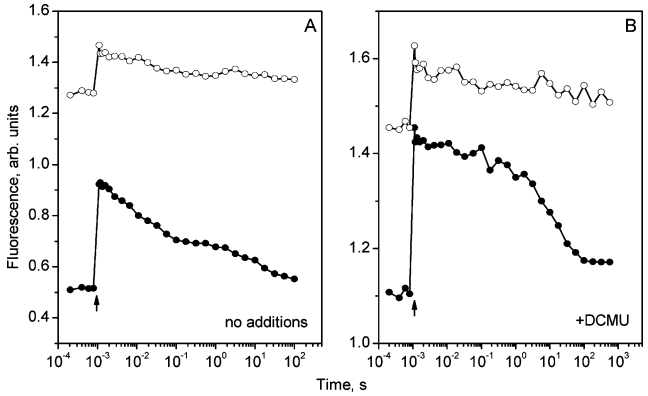

FIGURE 4: Flash-induced variable fluorescence decay kinetics measured from dark-adapted [PS II monomers/−Psb27] (●) and [PS II monomers/+Psb27] (○) in the absence (A) and presence (B) of 10 μM DCMU. The arrows indicate the position of the actinic flash. Each trace is an average of five measurements. Note the different time and fluorescence scales in (A) and (B).

The electron transfer between Q_A and Q_B in the two preparations was also investigated by flash-induced variable fluorescence at room temperature (Figure 4). Figure 4A shows the flash-induced fluorescence decay kinetics measured without any additional DCMU. The decay kinetics was very different between the [PS II monomers/−Psb27] and the [PS II monomers/+Psb27]. In the [PS II monomers/−Psb27] the fluorescence is characterized by a quite normal F_0 level. The flash resulted in a significant rise of the fluorescence, which decayed back to its original level with three kinetic phases (Table 2). The fluorescence decay was dominated by two phases with $\tau = 3.6$ and 46 ms, both typical for electron transfer from Q_A^- to Q_B. The fast phase ($\tau = 3.6$ ms) reflects electron transfer in centers where Q_B is present in its site while the intermediate phase ($\tau = 46$ ms) reflects electron transfer in PS II centers where the second quinone acceptor has to bind properly before electron transfer can occur. A significant part of the variable fluorescence decays much slower ($\tau = 13$ s), which reflects recombination between Q_A^- and the S_2 state in centers where forward electron transfer was not possible, presumably due to lack of Q_B. Taken together, these measurements show fast and efficient electron transfer from Q_A to Q_B in the [PS II monomers/−Psb27] that has an intact donor side (Scheme 1).

Table 2: Flash-Induced Fluorescence Decay Half-Times and Amplitudes with Standard Deviations for [PS II Monomers/−Psb27] and [PS II Monomers/+Psb27] in the Absence and Presence of 10 μM DCMU

PS II monomers	no DCMU				+DCMU		
	F_V/F_0	phase 1, ms (%)	phase 2, ms (%)	phase 3, s (%)	F_V/F_0	phase 1, ms (%)	phase 2, s (%)
[−Psb27]	0.80	3.6 ± 0.8 (34 ± 8)	46 ± 8 (33 ± 8)	13 ± 2 (33 ± 4)	0.30	84 ± 4 (21 ± 10)	16 ± 2 (79 ± 10)
[+Psb27]	0.14	nd[a]	23 ± 8 (51 ± 10)	>35 (49 ± 10)	0.12	25 ± 10 (30 ± 20)	>58 (70 ± 20)

[a] nd, not detected.

In the [PS II monomers/+Psb27] the situation is different. First, we observe that the F_0 level was much enhanced, resulting in a lower F_V/F_0 ratio (Figure 4A, Table 2). We interpret the abnormally high F_0 level to reflect the lower PS II reaction center content on a Chl basis, and it seems likely that some of these extra Chls (ca. 20 per PS II unit) are not well connected to the PS II reaction center in the energy transfer.

In addition, the decay kinetics of the flash-induced fluorescence was significantly altered in the [PS II monomers/+Psb27]. The fluorescence decay was dominated by intermediate decay kinetics ($\tau = 23$ ms, 51%) and very slow, almost nondecaying, kinetics in the remaining centers. The lack of a decay phase in the seconds time range, that would reflect Q_A^--S_2 recombination, is coherent with the lack of functional oxygen evolution. Even if we observe an intermediate decay kinetics ($\tau = 23$ ms, that could reflect forward electron transfer from Q_A^- to Q_B bound in a nonoptimal position), we have no indication of a fast phase reflecting forward electron transfer to Q_B in its normal site (compare $\tau = 3.6$ ms in the [PS II monomers/−Psb27], Table 2). Instead, a very similar intermediate phase ($\tau = 25$ ms; see below) dominates in our measurements with added DCMU where forward electron transfer is inhibited. Taken together, these observations indicate that recombination between Q_A^- and most probable $Y_Z^\bullet$ on the donor side is the origin for the intermediate ($\tau = 23$ ms) decay kinetics. Consequently, we conclude that forward electron transfer in the [PS II monomers/+Psb27] monomer is severely inhibited or blocked in the flash-induced fluorescence experiment. An additional conclusion is that $Y_Z^\bullet$ is functional in the [PS II monomers/+Psb27] although the OEC is absent.

At first sight it seems that our observations in the [PS II monomers/+Psb27] of a Q_A^--Fe^{2+}-Q_B^- EPR signal after illumination at 200 K and lack of forward electron transfer from Q_A^- after a single flash at room temperature are contradictory. However, this needs not be the case as the two measurements report on very different conditions. The applied illumination regime at 200 K is a phototrapping experiment where strong light is applied for a long time to the system. Under these circumstances, also intermediates which are formed in very low yield might be accumulated to an appreciable extent. An alternative option is that some reduced Q_B^- remains present in the fractions after the dark incubation so that reduction of only Q_A is enough to produce the Q_A^--Fe^{2+}-Q_B^- redox state necessary for the formation of the corresponding EPR signal. In contrast, the variable fluorescence measurement allows only one single charge separation to occur. If recombination reactions dominate in the system, there will be no observable or very small decay kinetics indicative of forward electron transfer although this might occur. We have represented this situation in Scheme 1 with a dotted arrow connecting Q_A and Q_B (indicating slow forward electron transfer) and a dashed arrow between Q_A and Y_Z (indicating an efficient recombination channel).

To conclude, our investigation of the function of the acceptor side in PS II indicates large differences between the two fractions. Although Psb27 does not bind in the close vicinity of Q_A or the acceptor side Fe^{2+}, we observed inhibited, or almost eliminated, forward electron transfer to Q_B in single flash experiments at room temperature in [PS II monomers/+Psb27]. Instead, recombination reactions with donor side components become dominating (see below). In addition, the fluorescence measurements suggest that the extra chlorophylls (ca. 20 per PS II center) in the [PS II monomers/+Psb27] are inefficiently connected to the P680.

Function of the Donor Side of PS II. Table 1 shows that the [PS II monomers/−Psb27] have a high O_2 evolution while almost no O_2 evolution was detected in [PS II monomers/+Psb27]. Steady-state oxygen evolution measurements are not informative of where the molecular lesion in the electron transfer chain occurs, and there might be several reasons for the lack of oxygen evolution. The functional integrity of the $CaMn_4$ cluster can be investigated by EPR spectroscopy, and a much studied spectroscopic probe is the multiline EPR signal from the $CaMn_4$ cluster in the S_2 state (*24*, *59*). Figure 5A (top) shows the S_2 multiline signal achieved by illumination at 200 K, obtained in the sample of [PS II monomers/−Psb27]. In this case illumination resulted in a large S_2 multiline signal [similar to what has been observed before in *T. elongatus* (*8*, *60*)], indicative of a structurally and functionally normal $CaMn_4$ cluster. In contrast our illumination of PS II monomers that contain Psb27 resulted in a spectrum completely devoid of the S_2 multiline signal (Figure 5A, lower).

Another spectral probe to the integrity of the PS II donor side is the so-called split EPR signals from $Y_Z^\bullet$ in magnetic interaction with the nearby $CaMn_4$ cluster (*23*, *26*, *58*, *61*, *62*) that can be induced by illuminating the sample at ultralow temperature while accumulating the EPR spectrum. In dark-adapted [PS II monomers/−Psb27] illumination at 6 K resulted in formation of a split EPR signal (Figure 5A, inset, top) as observed earlier in plants and *T. elongatus* (*23*, *26*, *58*, *61*, *62*). The signal induced in our preparation is slightly broader on the low-field side of $g = 2$ and has significant amplitude on the high-field side. This reflects that the spectrum is a mixture of the split S_1 signal and an analogous signal from the OEC in the S_0 state, the split S_0 signal (*23*, *26*, *62*). In the [PS II monomers/+Psb27] the same illumination regime did not result in the formation of any split EPR signal (Figure 5A, inset, bottom).

The complete absence of the S_2 multiline signal and the split S_1 signal, together with the absence of any EPR signal from Mn detectable in parallel mode EPR spectra from the [PS II monomer/+Psb27] fraction (not shown), supports our

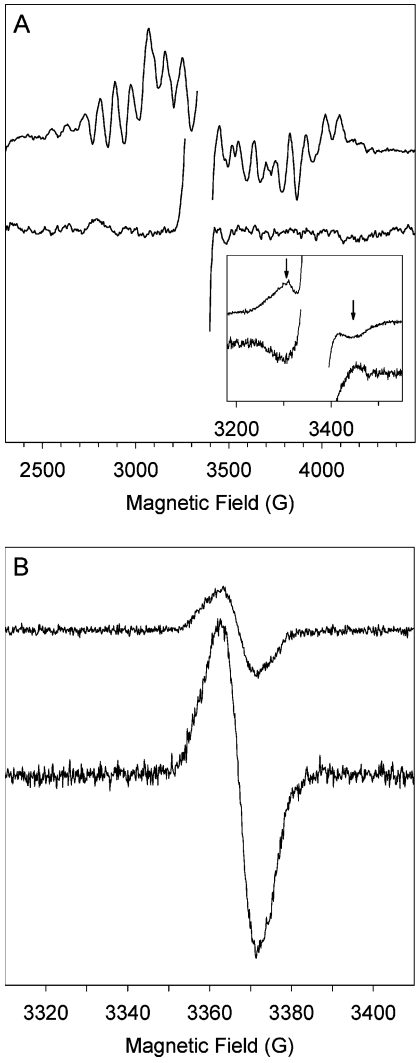

FIGURE 5: (A) Light minus dark difference EPR spectrum of the S_2 multiline signal from [PS II monomers/−Psb27] (top) induced by 6 min illumination at 200 K of a dark-adapted sample. The bottom spectrum is prepared in the same manner and shows the lack of any multiline signal in the [PS II monomers/+Psb27]. EPR conditions: $T = 7$ K; microwave power, 10 mW; modulation amplitude, 20 G; microwave frequency, 9.46 GHz. The inset shows the light minus dark difference spectrum of the split S_1-state EPR signal in [PS II monomers/−Psb27] (top). The arrows indicate the $g = 2.04$ and $g = 1.97$ peaks. The signal is induced by illumination at 6 K while accumulating the spectrum. The bottom spectrum is from the [PS II monomers/+Psb27], prepared in the same way as above, where no split signal is observed. EPR conditions for the inset: $T = 6$ K; microwave power, 25 mW; modulation amplitude, 20 G; microwave frequency, 9.46 GHz. (B) Light minus dark difference spectra of the induced $Chl^{+\bullet}$ signal in the same samples as in panel A ([PS II monomers/−Psb27] (top) and [PS II monomers/+Psb27] (bottom)). EPR conditions: $T = 15$ K; microwave power, 1.3 μW; modulation amplitude, 3.5 G; microwave frequency, 9.46 GHz. All spectra in the figure are normalized to the size of $Y_D^\bullet$ in the respective sample.

earlier conclusion (*3*) that the [PS II monomer/+Psb27] preparation lacks the $CaMn_4$ cluster (Scheme 1).

Illumination of PS II at low temperatures is known to result in oxidation of alternative electron donors together with, or instead of, the $CaMn_4$ cluster (*24*). Normally these donors involve oxidation of what is known as the Cyt b_{559}/carotenoid/Chl_Z pathway (*63*−*65*). Electron donation from these donors can be studied by EPR spectroscopy, and the result from our two preparations is shown in Figure 5B.

In the [PS II monomers/+Psb27], the EPR spectra after illumination at 200 K were dominated by the formation of the S_2 multiline (see above), but it also resulted in oxidation of a small amount of Cyt b_{559} (Figure 1A, top) and ca. 15% (on a $Y_D^\bullet$ basis) Chl_Z (Figure 5B, top). In the [PS II monomers/+Psb27] the effect of the illumination at 200 K was very different. The EPR spectra were dominated by the formation of a large radical signal, probably from a Chl radical, corresponding to about 60% of the centers (Figure 5B, bottom), while we could observe no oxidation of Cyt b_{559} [indicative of the absence of reduced Cyt (Figure 1A, bottom)], no induction of the S_2 multiline EPR signal (Figure 5A, bottom), or any buildup of stable $Y_Z^\bullet$. Consequently, the electron donor capabilities are seriously affected in [PS II monomers/+Psb27]. This is further corroborated by our measurements of flash-induced variable fluorescence (Figure 4B, Table 2). In the presence of DCMU the decay of the flash-induced variable fluorescence is normally dominated by recombination reactions between Q_A^- and donor side components in PS II. The decay kinetics consequently reports on the integrity of the PS II donor side. This is the case for the fluorescence decay for the [PS II monomers/−Psb27] where the recombination reactions between Q_A^- and the S_2 state, that occur in the seconds time range, totally dominate ($\tau = 15$ s, 79%).

In contrast, in the [PS II monomers/+Psb27] and in the presence of DCMU this seconds phase is completely lacking. Instead, the fluorescence decays much faster with kinetics ($\tau = 25$ ms, 30%) that strongly resembles recombination between Q_A^- and $Y_Z^\bullet$ in many studied systems from different origins (*66*−*70*). The remaining part of the flash-induced fluorescence is almost nondecaying in our time window ($\tau > 58$ s, 70%). This suggests that the flash results in the formation of electron donors that do not recombine well with Q_A^-, similar to what have been observed previously in other systems (*70*−*73*).

Taken together, our EPR and flash fluorescence measurements clearly show that the [PS II monomers/+Psb27] has a perturbed donor side; there is almost no oxygen evolution, no observable EPR signals from the $CaMn_4$ cluster, and enhanced electron donation from alternative electron donors, all reflecting the absence of the $CaMn_4$ cluster (Scheme 1).

CONCLUSIONS

We observe several differences in the function of redox components in [PS II monomers/+Psb27] and [PS II monomers/−Psb27]. The [PS II monomers/+Psb27] are characterized by an inactive (or totally absent) $CaMn_4$ cluster, slow and inefficient (but still possible) forward electron transfer from Q_A^- to Q_B, recombination between Q_A^- and $Y_Z^\bullet$ in a large fraction of the centers, and dominance of the low-potential form of Cyt b_{559}. These characteristics are quite similar to the situation in PS II lacking the $CaMn_4$ cluster in dark grown *Chlamydomonas reinhardtii* (*74*) and in hydroxylamine-washed PS II enriched membranes from spinach (*75*). In dark grown *C. reinhardtii*, PS II is partially functional except for the $CaMn_4$ cluster which has not yet been inserted via the so-called photoactivation reactions. PS II is inactive in oxygen evolution while the forward electron transfer from Q_A^- is significantly slowed down. Instead, Q_A^- (when formed) has been suggested to predominantly recom-

bine with $Y_Z^{\bullet}$ on the donor side of PS II. Cyt b_{559} is in the low-potential form. When the dark grown algae are illuminated, the $CaMn_4$ cluster is inserted through photoactivation simultaneously to activation of the forward electron transfer from Q_A^- to Q_B. Similar effects on forward electron transfer from Q_A^- (*75*) and a redox potential shift of Cyt b_{559} (*10*, *31*, *43*, *44*, *74*) have been observed when the $CaMn_4$ cluster is removed by Tris-washing or hydroxylamine washing of PS II membranes. It is thought that the removal of the $CaMn_4$ cluster resulted in a rise of the redox potential of Q_A^-, rendering electron transfer to Q_B less efficient (*75*). This redox potential shift of Q_A/Q_A^- was reversible upon rebinding of the $CaMn_4$ cluster.

The redox potential of Q_A/Q_A^- has not been determined in the dark grown cells of *C. reinhardtii* or in the [PS II monomers/+Psb27] from *T. elongatus* studied here. However, given the very similar chemistry observed between the different systems, it is highly likely that the redox potential of Q_A/Q_A^- is shifted to a higher potential also in [PS II monomers/+Psb27]. When the $CaMn_4$ cluster is inserted during the transition to the [PS II monomers/−Psb27], this results not only in activation of oxygen evolution but also in a lowering of the redox potential of Q_A/Q_A^- making forward electron transfer efficient. It is also likely that the observed shift in the redox potential of Cyt b_{559}, from the LP form in the absence of the $CaMn_4$ cluster to the HP form, is governed by the binding of the $CaMn_4$ cluster. Thus, it seems that many of the observed redox changes reflect the activation of the $CaMn_4$ cluster. This activation is, in turn, correlated to the dissociation of the Psb27 protein and the binding of the three extrinsic subunits, PsbO, PsbU, and PsbV, which stabilize the $CaMn_4$ cluster (*3*). Together, these effects point to a crucial role of Psb27 in the repair cycle for correct functional and structural assembly of the OEC in *T. elongatus*.

REFERENCES

1. Danielsson, R., Suorsa, M., Paakkarinen, V., Albertsson, P.-Å., Styring, S., Aro, E.-M., and Mamedov, F. (2006) Dimeric and monomeric organization of photosystem II: distribution of five distinct complexes in the different domains of the thylakoid membrane, *J. Biol. Chem. 281*, 14241−14249.
2. Dekker, J. P., and Boekema, E. J. (2005) Supramolecular organization of thylakoid membrane proteins in green plants, *Biochim. Biophys. Acta 1706*, 12−39.
3. Nowaczyk, M. M., Hebeler, R., Schlodder, E., Meyer, H. E., Warscheid, B., and Rögner, M. (2006) Psb27, a cyanobacterial lipoprotein, is involved in the repair cycle of photosystem II, *Plant Cell 18*, 1−11.
4. Zouni, A., Witt, H. T., Kern, J., Fromme, P., Krauss, N., Saenger, W., and Orth, P. (2001) Crystal structure of photosystem II from *Synechococcus elongatus* at 3.8 Å resolution, *Nature 409*, 739−743.
5. Ferreira, K. N., Iverson, T. M., Maghlaoui, K., Barber, J., and Iwata, S. (2004) Architecture of the photosynthetic oxygen-evolving center, *Science 303*, 1831−1838.
6. Loll, B., Kern, J., Saenger, W., Zouni, A., and Biesiadka, J. (2005) Towards complete cofactor arrangement in the 3.0 Å resolution structure of photosystem II, *Nature 438*, 1040−1044.
7. Kamiya, N., and Shen, J. R. (2003) Crystal structure of oxygen-evolving photosystem II from *Thermosynechococcus vulcanus* at 3.7-Å resolution, *Proc. Natl. Acad. Sci. U.S.A. 100*, 98−103.
8. Boussac, A., Sugiura, M., Inoue, Y., and Rutherford, A. W. (2000) EPR study of the oxygen evolving complex in His-tagged photosystem II from the cyanobacterium *Synechococcus elongatus*, *Biochemistry 39*, 13788−13799.
9. Fufezan, C., Zhang, C., Krieger-Liszkay, A., and Rutherford, A. W. (2005) Secondary quinone in photosystem II of *Thermosynechococcus elongatus*: semiquinone-iron EPR signals and temperature dependence of electron transfer, *Biochemistry 44*, 12780−12789.
10. Stewart, D. H., and Brudvig, G. W. (1998) Cytochrome b_{559} of photosystem II, *Biochim. Biophys. Acta 1367*, 63−87.
11. Shen, J.-R., Ikeuchi, M., and Inoue, Y. (1992) Stoichiometric association of extrinsic cytochrome c_{550} and 12 kDa protein with a highly purified oxygen-evolving photosystem II core complex from *Synechococcus vulcanus*, *FEBS Lett. 301*, 145−149.
12. Shen, J.-R., and Inoue, Y. (1993) Cellular localization of cytochrome c_{550}. Its specific association with cyanobacterial photosystem II, *J. Biol. Chem. 268*, 20408−20413.
13. Barber, J. (2003) Photosystem II: the engine of life, *Q. Rev. Biophys. 36*, 71−89.
14. Barber, J., Nield, J., Morris, E. P., Zheleva, D., and Hankamer, B. (1997) The structure, function and dynamics of photosystem two, *Physiol. Plant. 100*, 817−827.
15. Klinkert, B., Ossenbuhl, F., Sikorski, M., Berry, S., Eichacker, L., and Nickelsen, J. (2004) PratA, a periplasmic tetratricopeptide repeat protein involved in biogenesis of photosystem II in *Synechocystis* sp. PCC 6803, *J. Biol. Chem. 279*, 44639−44644.
16. Anbudurai, P. R., Mor, T. S., Ohad, I., Shestakov, S. V., and Pakrasi, H. B. (1994) The ctpA gene encodes the C-terminal processing protease for the D1 protein of the photosystem II reaction center complex, *Proc. Natl. Acad. Sci. U.S.A. 91*, 8082−8086.
17. Lax, J. E.-M., Arteni, A. A., Boekema, E. J., Pistorius, E. K., Michel, K.-P., and Rögner, M. (2007) Structural response of photosystem 2 to iron deficiency: characterization of a new photosystem 2-IdiA complex from the cyanobacterium *Thermosynechococcus elongatus* BP-1, *Biochim. Biophys. Acta* (in press).
18. Kashino, Y., Lauber, W. M., Carroll, J. A., Wang, Q., Whitmarsh, J., Satoh, K., and Pakrasi, H. B. (2002) Proteomic analysis of a highly active photosystem II preparation from the cyanobacterium *Synechocystis* sp. PCC 6803 reveals the presence of novel polypeptides, *Biochemistry 41*, 8004−8012.
19. Roose, J. L., and Pakrasi, H. B. (2004) Evidence that D1 processing is required for manganese binding and extrinsic protein assembly into photosystem II, *J. Biol. Chem. 279*, 45417−45422.
20. Chen, H., Zhang, D., Guo, J., Wu, H., Jin, M., Lu, Q., Lu, C., and Zhang, L. (2006) A Psb27 homologue in *Arabidopsis thaliana* is required for efficient repair of photodamaged photosystem II, *Plant Mol. Biol. 61*, 567−575.
21. Bricker, T. M., and Burnap, R. L. (2005) The extrinsic proteins of photosystem II, in *Photosystem II: The Light-Driven Water: Plastoquinone Oxidoreductase* (Wydrzynski, T. J., and Satoh, K., Eds.) pp 95−120, Springer, Dordrecht, The Netherlands.
22. Kuhl, H., Kruip, J., Seidler, A., Krieger-Liszkay, A., Bunker, M., Bald, D., Scheidig, A. J., and Rögner, M. (2000) Towards structural determination of the water-splitting enzyme. Purification, crystallization, and preliminary crystallographic studies of photosystem II from a thermophilic cyanobacterium, *J. Biol. Chem. 275*, 20652−20659.
23. Zhang, C., and Styring, S. (2003) Formation of split electron paramagnetic resonance signals in photosystem II suggests that $tyrosine_Z$ can be photooxidized at 5 K in the S_0 and S_1 states of the oxygen-evolving complex, *Biochemistry 42*, 8066−8076.
24. Miller, A. F., and Brudvig, G. W. (1991) A guide to electron paramagnetic resonance spectroscopy of photosystem II membranes, *Biochim. Biophys. Acta 1056*, 1−18.
25. Danielsson, R., Albertsson, P.-Å., Mamedov, F., and Styring, S. (2004) Quantification of photosystem I and II in different parts of the thylakoid membrane from spinach, *Biochim. Biophys. Acta 1608*, 53−61.
26. Havelius, K. G. V., Su, J.-H., Feyziyev, Y., Mamedov, F., and Styring, S. (2006) Spectral resolution of the split EPR signals induced by illumination at 5 K from the S_1, S_3, and S_0 states in photosystem II, *Biochemistry 45*, 9279−9290.
27. Mamedov, F., Rintamäki, E., Aro, E.-M., Andersson, B., and Styring, S. (2002) Influence of protein phosphorylation on the electron-transport properties of photosystem II, *Photosynth. Res. 74*, 61−72.
28. Styring, S., Virgin, I., Ehrenberg, A., and Andersson, B. (1990) Strong light photoinhibition of electrontransport in photosystem II. Impairment of the function of the first quinone acceptor, Q_A, *Biochim. Biophys. Acta 1015*, 269−278.
29. Vermaas, W. F. J., and Rutherford, A. W. (1984) EPR measurements on the effects of bicarbonate and triazine resistance on the acceptor side of photosystem II, *FEBS Lett. 175*, 243−248.

30. Mamedov, F., and Styring, S. (2003) Logistics in the life cycle of photosystem II: Lateral movement in the thylakoid membrane and activation of electron transfer, *Physiol. Plant. 119*, 328−336.
31. Magnuson, A., Rova, M., Mamedov, F., Fredriksson, P.-O., and Styring, S. (1999) The role of cytochrome b_{559} and tyrosine$_D$ in protection against photoinhibition during in vivo photoactivation of photosystem II, *Biochim. Biophys. Acta 1411*, 180−191.
32. Kaminskaya, O., Kurreck, J., Irrgang, K. D., Renger, G., and Shuvalov, V. A. (1999) Redox and spectral properties of cytochrome b_{559} in different preparations of photosystem II, *Biochemistry 38*, 16223−16235.
33. Thompson, L. K., Miller, A. F., Buser, C. A., de Paula, J. C., and Brudvig, G. W. (1989) Characterization of the multiple forms of cytochrome b_{559} in photosystem II, *Biochemistry 28*, 8048−8056.
34. Roncel, M., Boussac, A., Zurita, J. L., Bottin, H., Sugiura, M., Kirilovsky, D., and Ortega, J. M. (2003) Redox properties of the photosystem II cytochromes b_{559} and c_{550} in the cyanobacterium *Thermosynechococcus elongatus*, *J. Biol. Inorg. Chem. 8*, 206−216.
35. Shen, J.-R., and Inoue, Y. (1993) Binding and functional properties of two new extrinsic components, cytochrome *c*-550 and a 12-kDa protein, in cyanobacterial photosystem II, *Biochemistry 32*, 1825−1832.
36. Kirilovsky, D., Roncel, M., Boussac, A., Wilson, A., Zurita, J. L., Ducruet, J.-M., Bottin, H., Sugiura, M., Ortega, J. M., and Rutherford, A. W. (2004) Cytochrome c_{550} in the cyanobacterium *Thermosynechococcus elongatus*: study of redox mutants, *J. Biol. Chem. 279*, 52869−52880.
37. Kropacheva, T. N., Feikema, W. O., Mamedov, F., Feyziyev, Y., Styring, S., and Hoff, A. J. (2003) Spin conversion of cytochrome b_{559} in photosystem II induced by exogenous high potential quinone, *Chem. Phys. 294*, 471−482.
38. Hulsebosch, R. J. (1999) Magnetic and structural properties of electron transport cofactors in photosynthetic reaction centers, Ph.D. Thesis, Leiden University, Leiden, The Netherlands.
39. Petrouleas, V., and Diner, B. A. (1987) Light-induced oxidation of the acceptor-side Fe(II) of photosystem II by exogenous quinones acting through the Q_B binding site. I. Quinones, kinetics and pH-dependence, *Biochim. Biophys. Acta 893*, 126−137.
40. Aasa, R., Andréasson, L.-E., Styring, S., and Vänngård, T. (1989) The nature of the Fe(III) EPR signal from the acceptor-side iron in photosystem II, *FEBS Lett. 243*, 156−160.
41. Gadjieva, R., Mamedov, F., Renger, G., and Styring, S. (1999) Interconversion of low- and high-potential forms of cytochrome b_{559} in Tris-washed photosystem II membranes under aerobic and anaerobic conditions, *Biochemistry 38*, 10578−10584.
42. Bergström, J., and Franzén, L. G. (1987) Restoration of high-potential cytochrome *b*-559 in salt-washed photosystem II-enriched membranes as revealed by EPR, *Acta Chem. Scand., Ser. B 41*, 126−128.
43. Mizusawa, N., Ebina, M., and Yamashita, T. (1995) Restoration of the high potential form of cytochrome *b*-559 through the photoreactivation of Tris-inactivated oxygen-evolving center, *Photosynth. Res. 45*, 71−77.
44. Mizusawa, N., Miyao, M., and Yamashita, T. (1997) Restoration of the high-potential form of cytochrome *b*-559 by electron transport reactions through photosystem II in Tris-treated photosystem II membranes, *Biochim. Biophys. Acta 1318*, 145−158.
45. McNamara, V. P., and Gounaris, K. (1995) Granal photosystem II complexes contain only the high redox potential form of cytochrome *b*-559 which is stabilised by the ligation of calcium, *Biochim. Biophys. Acta 1231*, 289−296.
46. Hoganson, C. W., and Babcock, G. T. (1994) Photosystem-II, *Met. Ions Biol. Syst. 30*, 77−107.
47. Tommos, C., Madsen, C., Styring, S., and Vermaas, W. (1994) Point-mutations affecting the properties of tyrosine$_D$ in photosystem II. Characterization by isotopic labeling and spectral simulation, *Biochemistry 33*, 11805−11813.
48. Bender, C. J., Sahlin, M., Babcock, G. T., Barry, B. A., Chandrashekar, T. K., Salowe, S. P., Stubbe, J., Lindström, B., Petersson, L., Ehrenberg, A., and Sjöberg, B. M. (1989) An ENDOR study of the tyrosyl free-radical in ribonucleotide reductase from *Escherichia coli*, *J. Am. Chem. Soc. 111*, 8076−8083.
49. Barry, B. A., and Babcock, G. T. (1987) Tyrosine radicals are involved in the photosynthetic oxygen-evolving system, *Proc. Natl. Acad. Sci. U.S.A. 84*, 7099−7103.
50. Svensson, B., Vass, I., Cedergren, E., and Styring, S. (1990) Structure of donor side components in photosystem II predicted by computer modeling, *EMBO J. 9*, 2051−2059.
51. Rutherford, A. W., and Zimmermann, J. L. (1984) A new EPR signal attributed to the primary plastosemiquinone acceptor in photosystem II, *Biochim. Biophys. Acta 767*, 168−175.
52. Rutherford, A. W., Zimmermann, J. L., and Mathis, P. (1984) The effect of herbicides on components of the PS II reaction centre measured by EPR, *FEBS Lett. 165*, 156−162.
53. Demeter, S., Goussias, C., Bernat, G., Kovacs, L., and Petrouleas, V. (1993) Participation of the $g = 1.9$ and $g = 1.82$ EPR forms of the semiquinone-iron complex, $Q_A^- \cdot Fe^{2+}$ of photosystem II in the generation of the Q and C thermoluminescence bands, respectively, *FEBS Lett. 336*, 352−356.
54. Sinning, I., Michel, H., Mathis, P., and Rutherford, A. W. (1989) Characterization of four herbicide-resistant mutants of *Rhodopseudomonas viridis* by genetic analysis, electron paramagnetic resonance, and optical spectroscopy, *Biochemistry 28*, 5544−5553.
55. McDermott, A. E., Yachandra, V. K., Guiles, R. D., Cole, J. L., Dexheimer, S. L., Britt, R. D., Sauer, K., and Klein, M. P. (1988) Characterization of the manganese O_2-evolving complex and the iron-quinone acceptor complex in photosystem II from a thermophilic cyanobacterium by electron paramagnetic resonance and X-ray absorption spectroscopy, *Biochemistry 27*, 4021−4031.
56. Hallahan, B. J., Ruffle, S. V., Bowden, S. J., and Nugent, J. H. A. (1991) Identification and characterisation of EPR signals involving Q_B semiquinone in plant photosystem II, *Biochim. Biophys. Acta 1059*, 181−188.
57. Corrie, A. R., Nugent, J. H. A., and Evans, M. C. W. (1991) Identification of EPR signals from the states $Q_A^{\bullet-}Q_B^{\bullet-}$ and $Q_B^{\bullet-}$ in photosystem II from *Phormidium laminosum*, *Biochim. Biophys. Acta 1057*, 384−390.
58. Zhang, C., Boussac, A., and Rutherford, A. W. (2004) Low-temperature electron transfer in photosystem II: a tyrosyl radical and semiquinone charge pair, *Biochemistry 43*, 13787−13795.
59. Dismukes, G. C., and Siderer, Y. (1981) Intermediates of a polynuclear manganese center involved in photosynthetic oxidation of water, *Proc. Natl. Acad. Sci. U.S.A. 78*, 274−278.
60. Boussac, A., Kuhl, H., Un, S., Rögner, M., and Rutherford, A. W. (1998) Effect of near-infrared light on the S_2-state of the manganese complex of photosystem II from *Synechococcus elongatus*, *Biochemistry 37*, 8995−9000.
61. Nugent, J. H., Muhiuddin, I. P., and Evans, M. C. (2002) Electron transfer from the water oxidizing complex at cryogenic temperatures: the S_1 to S_2 step, *Biochemistry 41*, 4117−4126.
62. Petrouleas, V., Koulougliotis, D., and Ioannidis, N. (2005) Trapping of metalloradical intermediates of the S-states at liquid helium temperatures. Overview of the phenomenology and mechanistic implications, *Biochemistry 44*, 6723−6728.
63. Vrettos, J. S., Stewart, D. H., de Paula, J. C., and Brudvig, G. W. (1999) Low-temperature optical and resonance Raman Spectra of a carotenoid cation radical in photosystem II, *J. Phys. Chem. B 103*, 6403−6406.
64. Hanley, J., Deligiannakis, Y., Pascal, A., Faller, P., and Rutherford, A. W. (1999) Carotenoid oxidation in photosystem II, *Biochemistry 38*, 8189−8195.
65. Faller, P., Pascal, A., and Rutherford, A. W. (2001) β-Carotene redox reactions in photosystem II: electron transfer pathway, *Biochemistry 40*, 6431−6440.
66. Conjeaud, H., and Mathis, P. (1980) The effects of pH on the reductions kinetics of *P*-680 in Tris-treated chloroplasts, *Biochim. Biophys. Acta 590*, 353−359.
67. Conjeaud, H., and Mathis, P. (1986) Electron-transfer in the photosynthetic membrane—Influence of pH and surface-potential on the P-680 reduction kinetics, *Biophys. J. 49*, 1215−1221.
68. Renger, G., and Voelker, M. (1982) Studies on the proton release pattern of the donor side of system II: Correlation between oxidation and deprotonization of donor D_1 in Tris-washed inside-out thylakoids, *FEBS Lett. 149*, 203−207.
69. Schlodder, E., and Meyer, B. (1987) pH dependence of oxygen evolution and reduction kinetics of photooxidized chlorophyll a_{II} (P-680) in photosystem II particles from *Synechococcus* sp., *Biochim. Biophys. Acta 890*, 23−31.
70. Mamedov, F., Sayre, R. T., and Styring, S. (1998) Involvement of histidine 190 on the D1 protein in electron/proton transfer reactions on the donor side of photosystem II, *Biochemistry 37*, 14245−14256.

71. Ghirardi, M. L., Lutton, T. W., and Seibert, M. (1996) Interactions between diphenylcarbazide, zinc, cobalt, and manganese on the oxidizing side of photosystem II, *Biochemistry 35*, 1820−1828.
72. Dekker, J. P., Van Gorkom, H. J., Wensink, J., and Ouwehand, L. (1984) Absorbance difference spectra of the successive redox states of the oxygen-evolving apparatus of photosynthesis, *Biochim. Biophys. Acta 767*, 1−9.
73. Metz, J. G., Nixon, P. J., Rögner, M., Brudvig, G. W., and Diner, B. A. (1989) Directed alteration of the D1 polypeptide of photosystem II: Evidence that tyrosine-161 is the redox component, Z, connecting the oxygen-evolving complex to the primary electron donor, P680, *Biochemistry 28*, 6960−6969.
74. Rova, M., Mamedov, F., Magnuson, A., Fredriksson, P.-O., and Styring, S. (1998) Coupled activation of the donor and the acceptor side of photosystem II during photoactivation of the oxygen evolving cluster, *Biochemistry 37*, 11039−11045.
75. Johnson, G. N., Rutherford, A. W., and Krieger, A. (1995) A change in the midpoint potential of the quinone Q_A in photosystem II associated with photoactivation of oxygen evolution, *Biochim. Biophys. Acta 1229*, 202−207.

BI7000399